A distributed approach to model-predictive control of radiant comfort delivery systems in office spaces with localized thermal environments

Jaewan Joe[1,3], Panagiota Karava[1,3*], Xiaodong Hou[2,3], Yingying Xiao[2,3], Jianghai Hu[2,3]

[1]*Lyles School of Civil Engineering, Purdue University, 550 Stadium Mall Dr., West Lafayette, Indiana, USA 47907*

[2]*School of Electrical and Computer Engineering, Purdue University, 550 Stadium Mall Dr., West Lafayette, Indiana, USA 47907*

[3]*Center for High Performance Buildings, Ray W. Herrick Laboratories, 140 S. Martin Jischke Dr.,West Lafayette, Indiana, USA 47907*

** Corresponding author. Tel.: 765-494-4573*
E-mail: pkarava@purdue.edu

Abstract

This paper introduces a new multi-agent system approach to optimal control of high performance buildings and presents algorithms for both distributed system identification and distributed model predictive control (DMPC). For the system identification, each thermal zone is divided into sub-systems, and a parameter set for each sub-system is first estimated individually, and then integrated into an inverse model for the whole thermal zone using the dual decomposition algorithm. For the DMPC, a distributed optimization algorithm inspired by the Proximal Jacobian Alternating Direction Method of Multipliers (PJ-ADMM) is deployed and multiple MPCs run iteratively while exchanging control input information until they converge. The developed algorithms are tested using field data from an occupied open-plan office space with a radiant floor system with distributed sensing, control, and data communication capabilities for localized comfort delivery. With this tractable approach, agents solve individual optimization problems in parallel, through information exchange and broadcasting, with a smaller scale of the input and constraints, facilitating optimal solutions with improved efficiency that are scalable to different building applications. Using a data-driven model and weather forecast, the DMPC controller is implemented to optimize the operation of an air-cooled chiller while providing different operative temperature bounds for each radiant floor loop. The radiant comfort delivery system with predictive control is capable of providing localized thermal environments while achieving significant energy savings. For the system and climate under consideration, results from the building operation during the cooling season, show 27% reduction in electricity consumption compared to baseline feedback control.

Keywords: Radiant floor cooling system, Distributed optimization, MPC implementation, Thermal environment control

1 Introduction

1.1 New technology for thermal environment control

In recent years, following the development of low-cost sensing, smart devices and the Internet of Things (IoT) technology, the potential for spatial control granularity is extended and conventional zone control with a single set-point is evolving to occupancy prediction-based [1-5] or personalized [6-9] control. At the same time, the role of building occupants is being transformed to "service users" who participate, decide, provide feedback, and communicate with building systems [10, 11]. Space conditioning is provided when zones are occupied [12] to achieve energy savings and satisfy occupants with diverse thermal preferences [13-16]. Building systems and devices are beginning to embed analytical software for communications and enhanced control functions. To provide thermal environments with higher resolution, new smart devices might be deployed in building systems, and eventually transform the configuration of Building Management Systems (BMS) fundamentally [17]. Also, the connectivity between building occupants and those devices is extended with sensing and computing abilities of cell phones or single board computers (e.g., Raspberry Pi) and wireless communication methods (e.g., ZigBee or Bluetooth), and it is geared towards the new BMS configuration [18].

Open-plan spaces have become a new trend in office buildings, and with the availability of data from sensors, smart devices and occupants, smart comfort delivery can provide significant opportunities for energy savings [6, 7] as conditioning is deployed where it is actually needed. When implemented in a building, it is expected to enable an expansion of the temperature setpoints in unoccupied spaces, resulting in energy savings that can be over 20% compared to baseline approaches depending on the building and climate [19].

Despite the advent of new technology for distributed sensing, data communication, and information processing, advantages are confined to typical HVAC systems enhanced with new control functions [20, 21]. Additional benefits could be leveraged using systems that facilitate the delivery of personalized or localized thermal environments [22, 23]. Various types of HVAC systems that provide different thermal conditions for an individual occupant (known as Task-ambient Conditioning (TAC) or Personal Environmental Control (PEC)) have been studied up to date [24-26]. These include a chair [6, 7] and desk diffusers [27, 28] or heating panels [27, 29] for conditioning body parts. However, heating is much easier to implement than cooling, primarily due to the problem of dealing with rejected heat while infrared heaters may create discomfort due to thermal asymmetry. Also, with only few exemptions [9, 30] TAC or PEC systems have operated independently from the building's environmental control. At the same time, different approaches with building-integrated HVAC such as under-plenum air distribution (UFAD) [31] and

thermally-activated building systems (TABS), such as radiant floor heating system [32], have been explored focusing on sizing the cooling capacity. Although, it is challenging for building-integrated HVAC such as VAV diffusers, UFAD, and radiant systems to reach the resolution of an individual occupant, localized thermal zones can be used to facilitate different occupancy schedules and occupants preferring warm, cool or accepting a wider range of thermal conditions [10, 16].

1.2 Radiant floor system

Radiant floor heating and cooling has been investigated for a long time and its superior performance in terms of energy saving and improved comfort have been revealed in many studies [33-38]. From a localized thermal management perspective, radiant systems with distributed sensing and control loops, are capable of providing different thermal environments by selectively conditioning a slab section as opposed to air systems in which the air is mixed easily in an open space. This leads to better occupant comfort as different thermal preferences can be simultaneously met.

However, conventional feedback strategies for radiant floor systems are limited in terms of providing the anticipated benefits for building climate control, due to the large thermal capacity. Model predictive control (MPC) is considered as a promising solution for this system as shown in literature [39-42]. In this approach, operation is optimized using information for the specific building and climate through an estimated process model to predict the future evolution of the system, while incorporating the most up-to-date information on weather forecast and system dynamics [43, 44]. The benefits of such systems can be augmented by incorporating in sensing and control frameworks the building occupants, i.e. their schedule and thermal preferences, to facilitate localized comfort delivery in open-plan office spaces.

On the other hand, MPC requires high engineering cost for developing control-oriented building models which is referred to as system identification. In the case of high performance buildings, in which the requirements for thermal environments with higher resolution and energy savings are increased, complex building designs bring additional challenges for developing building models and typical parameter estimation techniques may become infeasible [45]. Moreover, as the building scale becomes large or finer control granularity is needed, the dimension of control variables is increased; thereby the computation cost to find optimal solutions is also higher, which makes the MPC problem intractable [46, 47]. In this regard, scalable distributed algorithms need to be developed that are applicable to building applications for smart thermal environment control and flexible to different scales of the system for the generalization.

1.3 Multi-agent system

For better performance in buildings with complex systems, it is possible to utilize the modularity of their sub-systems to deploy plug-and-play operation strategy that improve efficiency, flexibility and scalability. For instance, distributed optimization method enables this realization for the control of coupled but separable sub-systems that are jointly optimized. In order to coordinate the solution of the sub-problems,

a network of intelligent agents is formed. In multi-agent networks, agents are equipped with the capability of sensing, information processing and communication [48-51]. This approach, known as multi-agent DMPC, is a tractable solution for large-scale problems due to the reduced computation cost with less decision variables for each local optimization problem, the feasibility to find an optimal solution by focusing on one objective, the possibility to easily adapt model parameters with respect to the varying environments, and the robustness in terms of whole system operation in the case of fault or failure of subsystems. In previous studies that utilize the multi-agent approach for building control applications, agents are defined in many different ways. For example, in some cases definitions are made according to the HVAC source, namely electrical, heating and cooling agents [52, 53]. Other definitions are based on the control hierarchy such as central, local [54], or producer, distributor, consumer [55]. Finally, agents may also represent building occupants [56-58]. Although theoretical approaches for agent definitions exist [48], previous research mainly focuses on specific examples or case studies.

1.4 Distributed optimization

In controls community, the concept of DMPC was developed to simplify complex control problems and has been investigated for a long time. As a result, several theoretical DMPC approaches exist. An extensive overview and classification is presented in [50]. Other comprehensive reviews exist with application to power [59] and chemical system [60] applications. In these studies, the general DMPC structure is discussed and compared to centralized or decentralized MPC approaches, by presenting the goal of decomposition [59] and reviewing the evolution of theoretical approaches [60]. With regards to the details of the optimization problem and its decomposition, a well-organized and comprehensive classification based on the couplings in cost function and constraints between the sub-systems is discussed in [49] along with various decomposition algorithms.

In building applications, Bender's decomposition, one of the initial decomposition methods, was used for a multi-zone heating case with central radiant floor and individual convectors [61]. A classical but more recent decomposition method, the primal decomposition, was utilized for solving a resource allocation problem using a coordinator between the grid and a multi-zone building [62] and a building cluster [63]. The dual decomposition method has been implemented on a multi-zone building application with an Air Handling Unit (AHU) and multiple Variable Air Volume (VAV) boxes [64-66]. This approach was also applied to a distributed estimation problem [45] as a negotiation strategy and was demonstrated using a case study with an open-plan office space with a radiant floor system. However, dual decomposition is not guaranteed to converge for certain problems whose objective functions are not strictly convex, and requires a fine tuning of step-size parameters. On the other hand, the alternating directions of multipliers (ADMM) is another primal-dual based method that utilizes an extra quadratic penalty term when formulating the Lagrangian function, which has much better convergence behavior compared to dual decomposition.

ADMM has been used for several case studies of multi-zone buildings including HVAC component coordination [67] and demand response [68] and monthly optimization to reduce demand charge [46]. Nevertheless, the conventional ADMM method is based on a sequential update that requires the order and priority of the agents. Very recently a Proximal Jacobian ADMM (PJ ADMM) method at which parallel computation is available was developed and implemented for a simulation case study with a single zone served with several roof top units (RTUs) [69]. In this paper, the DMPC algorithm is developed based on the PJ ADMM, and implemented to an actual building to demonstrate optimal performance under realistic conditions.

1.5 Contributions of this work

The objective of this study is to develop and demonstrate a new multi-agent system approach to tractable optimal control of buildings. The work presented in this paper aims to address issues related to the modeling complexity and growing control input dimension in office buildings with high resolution thermal environments. The developed distributed system identification and MPC algorithms, facilitate the information exchange between agents, and they are efficient, with reduced computation cost, and scalable to different building applications.

With an actual open-plan office space with radiant comfort delivery as test-bed, distributed system identification is deployed, in which each building system (agent) is estimated individually, and then integrated to one model through the information exchange and negotiation between neighboring agents. Using this data-driven model along with distributed sensing, control, and data communication, a new DMPC algorithm inspired by the Proximal Jacobian Alternating Direction Method of Multipliers (PJ-ADMM) method is implemented to demonstrate the energy saving potential and comfort improvement of the smart thermal environment control system.

In this paper, Section 2 presents the new methodology for the distributed modelling and control. The DMPC implementation in an actual test-bed in discussed in Section 3. The main findings and conclusions are outlined in Section 4.

2 Methodology

2.1 Distributed system identification algorithm

The first step in MPC is developing a data-driven model. In this work, a grey-box approach is adopted for the building model (Eq. (1)). The one-step ahead temperature (x[n+1]) is a linear function of the current temperature (x[n]), the exogenous input (w[n]) and control input (u[n]). The state and input matrix (A_d and B_d) consist of estimate parameters including the thermal capacity and resistance, as well as the coefficient multiplied to the heat flux input for the transmitted solar radiation and internal heat gain. The temperature trajectory ($\mathbf{X}$) is a linear function of the matrix ($\mathbf{\Omega_x}$), lower block triangular matrix ($\mathbf{\Omega_w}$

and $\mathbf{\Omega_u}$), the initial state vector ($\mathbf{X_0}$), and the exogenous input ($\mathbf{w}$) and control input vector ($\mathbf{u}$), as shown in Eq. (2). The control input and temperature trajectories are in an explicit linear relation, which is a suitable form for implementation in the optimization algorithm.

$$x[n+1] = A_d x[n] + B_{d,w} w[n] + B_{d,u} u[n] \quad (1)$$

$$\underbrace{\begin{bmatrix} x[1] \\ x[2] \\ \vdots \\ x[n] \end{bmatrix}}_{\mathbf{X}} = \underbrace{\begin{bmatrix} A_d \\ {A_d}^2 \\ \vdots \\ {A_d}^n \end{bmatrix}}_{\mathbf{\Omega_x}} \underbrace{x[0]}_{\mathbf{X_0}} + \underbrace{\begin{bmatrix} B_{d,w} & 0 & \cdots & 0 \\ A_d B_{d,w} & B_{d,w} & \cdots & 0 \\ \vdots & \vdots & \ddots & \vdots \\ {A_d}^{n-1} B_{d,w} & {A_d}^{n-2} B_{d,w} & \cdots & B_{d,w} \end{bmatrix}}_{\mathbf{\Omega_w}} \underbrace{\begin{bmatrix} w[0] \\ w[1] \\ \vdots \\ w[n-1] \end{bmatrix}}_{\mathbf{w}}$$
$$+ \underbrace{\begin{bmatrix} B_{d,u} & 0 & \cdots & 0 \\ A_d B_{d,u} & B_{d,u} & \cdots & 0 \\ \vdots & \vdots & \ddots & \vdots \\ {A_d}^{n-1} B_{d,u} & {A_d}^{n-2} B_{d,u} & \cdots & B_{d,u} \end{bmatrix}}_{\mathbf{\Omega_u}} \underbrace{\begin{bmatrix} u[0] \\ u[1] \\ \vdots \\ u[n-1] \end{bmatrix}}_{\mathbf{u}} \quad (2)$$

The objective function for the parameter estimation is the summation of the deviation between the measurement and model prediction. Each element in A_d and B_d matrix has a form of multiplication of the estimate parameters; thus, the optimization problem (Eq. 3) is nonlinear. Initial values are set based on information from the drawing and building energy simulation programs [70, 71] and are used for setting lower and upper bounds for the estimate parameter based on the approach described in Joe and Karava, 2016 [45]. To solve this constrained nonlinear optimization problem, Fmincon with active-set algorithm is used in Matlab environment [72].

$$\begin{aligned} &\text{minimize} \sum_{k=1}^{n} (\hat{y}[k] - y[k])^2 \\ &\text{where:} \\ &x[n+1] = A_d(\theta) x[n] + B_d(\theta) u[n] \\ &\hat{y}[n] = C_d X[n] \end{aligned} \quad (3)$$

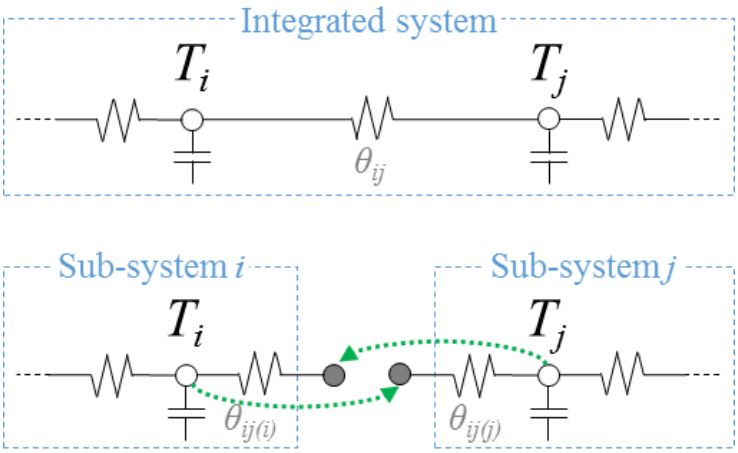

Figure 1. Generic example of distributed system identification

Figure 1 represents a generic distributed system identification example in which the zone model (referred to as an integrated model) is split into two sub-system models represented by agents *i* and *j*. The heat flux input is not considered for this generic example. In our approach, system identification is performed locally on each agent while neighboring agents exchange measured information such as their temperature trajectory. Temperature trajectories from the sensor of each adjacent agent are used as a boundary temperature for the agent (as illustrated in Figure 1 using arrows). Each zone agent minimizes the deviation between the calculated prediction and measured trajectories from its own sensor; and thereby the two shared parameters ($\theta_{ij(i)}$ and $\theta_{ij(j)}$, which are thermal resistances in this example) between the agents are different. In the next step, these deviated estimate parameters converge to the same value using the dual decomposition method (Algorithm 1). θ_i and θ_j are estimate parameters for agents *i* and *j*. The objective function minimizes the deviation between the prediction and measurement, *g* in Algorithm 1, and it is augmented by the Lagrangian term ($\lambda_{ij}\theta_{ij}$). The Lagrangian multiplier (λ_{ij}) is updated in each iteration *k*, with the deviation of two estimate parameters ($\theta_{ij(i)} - \theta_{ij(j)}$).The iteration stops when the two estimate parameters converge to the same value. The details of this approach are described in Joe and Karava 2016 [45].

Algorithm 1

while $\theta_{ij(i)}^{k+1} = \theta_{ij(j)}^{k+1}$

$$\theta_i^{k+1} = \underset{\theta_i^k}{\operatorname{argmin}} \left(g_i(\theta_i^k) + \lambda_{ij}^k \theta_{ij(i)}^k \right)$$

$$\theta_j^{k+1} = \underset{\theta_j^k}{\operatorname{argmin}} \left(g_j(\theta_j^k) - \lambda_{ij}^k \theta_{ij(j)}^k \right)$$

$$\lambda_{ij}^{k+1} = \lambda_{ij}^k + \mu_{ij} \left(\theta_{ij(i)}^{k+1} - \theta_{ij(j)}^{k+1} \right)$$

end

2.2 Distributed MPC algorithm

In thermal environment control of buildings, the objective function is the HVAC energy consumption. The decision variable **u**, which is the control input to the model, is the trajectory of Part Load Ratio (PLR) in a given prediction horizon. f_{HVAC} represents the electricity consumption of the HVAC source, which is a convex function when the PLR is the control input. The dimension of the trajectory is increased with the number of zones or systems that are connected to the shared HVAC source. The centralized MPC algorithm is formulated as a convex optimization problem (Eq. 4) with several linear inequality constraints. The first constraint represents the temperature bound of the conditioned zone; $\mathbf{T_{bound}}$ is the upper or lower temperature bound, and $\mathbf{C_T}$ is the matrix multiplied to all states to extract the target temperature states. Additional bounds can be used for certain states of the system, for example, slab temperatures in radiant systems. The last constraint is set for the capacity of the HVAC source. $\mathbf{\Omega}$ represents the predefined matrices as shown in Eq. 2.

$$\begin{aligned} &\min f_{HVAC}\left(\begin{bmatrix}\mathbf{I} & \mathbf{I} & \cdots\end{bmatrix}\begin{bmatrix}\mathbf{u_i}\\ \mathbf{u_{i+1}}\\ \vdots\end{bmatrix}\right) \\ &s.t.\begin{bmatrix}\mathbf{C_T}\cdot\mathbf{\Omega_{u,i}} & \mathbf{C_T}\cdot\mathbf{\Omega_{u,i+1}} & \cdots\\ \vdots & \vdots & \cdots\\ \mathbf{I} & \mathbf{I} & \ddots\end{bmatrix}\begin{bmatrix}\mathbf{u_i}\\ \mathbf{u_{i+1}}\\ \vdots\end{bmatrix}\leq\begin{bmatrix}\mathbf{T_{bound}}-\mathbf{C_T}\cdot\left(\mathbf{\Omega_T}\cdot\mathbf{T_0}+\mathbf{\Omega_w}\cdot\mathbf{w}\right)\\ \vdots\\ \mathbf{u_{max}}\end{bmatrix} \end{aligned} \quad (4)$$

Algorithm 2 is the distributed MPC used in our study. It is inspired by the Proximal Jabcobian Alternating Direction Method of Multipliers (PJ-ADMM) [69], which is a variant of the classical ADMM method. The optimization in each controller is regulated with a proximal term and the control inputs of other agents (neighbors) are transferred from the previous iteration for parallel computing. Multiple optimizations for each agent (referred to as agent *i*) run in parallel until the convergence criteria are satisfied. In this formulation, the coupled cost is decomposed by fixing the control input of other agents ($\sum \mathbf{u}_{neighbors}^{k-1}$) so the dimension of the control input ($\mathbf{u}_i^k$) is reduced according to the number of agents. Decomposition is feasible as information from other agents is transferred from the previous iteration (referred to as step *k-1*). This enables parallel optimization, which would not be otherwise possible, as the objective function is evaluated with all control input trajectories from other agents. The same inequality constraints with centralized MPC are set.

Algorithm 2

1: initialize $\left(\mathbf{u}_\mathbf{i}^0,\ \ldots,\boldsymbol{\phi}_\mathbf{i}^0,\ \ldots\right)$

2: repeat following optimizations in parallel

$$\left|\begin{array}{l}
3:\ \mathbf{u}_\mathbf{i}^k = \arg\min_{\mathbf{u_i}}\left(f_{HVAC}\left(\mathbf{u_i} + \sum \mathbf{u}_{neighbors}^{k-1}\right) + \boldsymbol{\phi}_\mathbf{i}^{k-1}\left\|\mathbf{u_i} - \mathbf{u}_\mathbf{i}^{k-1}\right\|^2\right) \\
4:\ s.t. \begin{bmatrix} \mathbf{C_{T,i}}\cdot\boldsymbol{\Omega}_\mathbf{u,i} \\ \vdots \\ \mathbf{1} \end{bmatrix}\cdot\mathbf{u}_\mathbf{i}^k \le \begin{bmatrix} \mathbf{T_{bound}} - \mathbf{C_{T,i}}\cdot\left(\boldsymbol{\Omega}_\mathbf{T}\cdot\mathbf{T_0} + \boldsymbol{\Omega}_\mathbf{w}\cdot\mathbf{w} + \sum \boldsymbol{\Omega}_{neighbors}\cdot\mathbf{u}_{neighbors}^{k-1}\right) \\ \vdots \\ \mathbf{u_{max}} - \sum \mathbf{u}_{neighbors}^{k-1} \end{bmatrix} \\
5:\ \boldsymbol{\phi}_\mathbf{i}^k = \boldsymbol{\phi}_\mathbf{i}^{k-1} + \sigma\left|\mathbf{u}_\mathbf{i}^k - \mathbf{u}_\mathbf{i}^{k-1}\right| \\
\vdots
\end{array}\right.$$

6: until $\max\left(\left\|\begin{bmatrix} \mathbf{u}_\mathbf{i}^k \\ \mathbf{u}_\mathbf{i+1}^k \\ \vdots \end{bmatrix} - \begin{bmatrix} \mathbf{u}_\mathbf{i}^{k-1} \\ \mathbf{u}_\mathbf{i+1}^{k-1} \\ \vdots \end{bmatrix}\right\|\right) \le \varepsilon_{stop}$

Each agent searches for the optimal control inputs while exchanging information with other agents. The regulation term with multiplier $\boldsymbol{\phi}_\mathbf{i}$ is added to the objective function to encourage the convergence of the iterated control inputs. This multiplier is a vector which is updated with the deviation of two control input trajectories. In initial iterations, it is small so each agent calculates its objective function with less restriction. Then, as the iteration evolves, the regulation term becomes large and, the algorithm converges when the maximum value of the deviation of two control input trajectories is smaller than the stop criteria, ε_{stop}. The way Algorithm 2 updates the regulation term ($\boldsymbol{\phi}_\mathbf{i}$) helps speed up the convergence speed, however, it comes at the price of sacrificing optimality performance.

3 Application to optimal building climate control

In this section, we present the application of our multi-agent system approach into an actual test-bed. First, we describe the test-bed and the system identification for developing the building model. Then, we provide details for the DMPC implementation including the HVAC system, exogenous inputs and constraints, and we describe the data communication process. Finally, we discuss the performance of the DMPC controller with regards to thermal environment control and energy saving potential.

3.1 Test-bed

The test-bed used in this study is an open-plan office space (9.9 m by 10.5 m) in a university building at Purdue campus that can host up to 20 occupants. An exterior view of the building is shown in

Figure 2(top). The main features of the test-office are a radiant floor slab and a south-facing double façade system. The radiant floor has been constructed to provide cooling and heating with sensing capabilities, since it is a research Living Laboratory (Figure 2(middle)). It includes 10 parallel loops in the concrete slab, a heat exchanger and a pump (Figure 2(bottom)). Steam and chilled water is delivered to the heat exchanger from the campus plant. Temperature sensors (ACI, A/TT1K-LTS, ±0.3℃) are embedded in each concrete slab and in the heat exchanger to monitor the supply and return water temperature. A turbine-type flow meter (ONICOM, F-1110, ±1%) is installed between the loops and the heat exchanger.

For the DMPC implementation, we explore the potential of the system to provide localized thermal conditioning and we present results for the cooling season. For this purpose, the room is divided into four thermal zones corresponding to four sections of the radiant floor as shown in Figure 2 (middle). Each floor section consists of two pipe loops that are controlled together. RTD sensors (Digi-Key, 10K ohm, 1%) and thermocouples (Omega, T-type, ±0.5℃) are installed in each section (0.6 m height from the floor and on floor) to measure the air and slab surface temperatures (Figure 2(middle)). Ultrasonic flow meters (TUF-2000M, ±1%) and thermocouples (Omega, T-type, ±0.5℃) are attached and inserted at each pipe loop to capture the cooling rate for each section (Figure 3). The room has four wall diffusers for ventilation that are connected to an Air Handling Unit (AHU). The vents and fan of the double façade were kept closed during this study. A standard BMS is available through the installed Tridium JACE controllers and Niagara/AX software framework [73].

3.2 Building model

The system identification experiment was conducted using the four room sections from the south to north direction as shown in Figure 2 (middle). To ensure sufficient excitation, cooling was provided to alternate floor sections for about six to twelve hours and the minimum surface temperature for the floor was 18~19℃. The room was occupied most of the day time so the air temperature was maintained with the ventilation system between 22 and 24℃.

The typical (centralized) estimation approach is not feasible for this system due to the large number of estimate parameters and the different magnitude of state trajectories in each sub-system including the double façade, the four thermal zones and the radiant floor (Figure 4). Therefore, a distributed system identification approach is deployed with six sub-system models (represented by six agents) representing the four thermal zones, the radiant floor and the double façade. The six sub-system models are initially estimated in parallel, reducing the scale of the estimation problem, and then integrated in a plug-and-play manner. The structure of the integrated model (Figure 4(a)) consists of 17 states and 27 resistances (17C27R) with one boundary temperature which is the outdoor air temperature. Figure 4 shows only a portion of the model by excluding the repeated structure for simplicity. Resistances between the air nodes are fixed

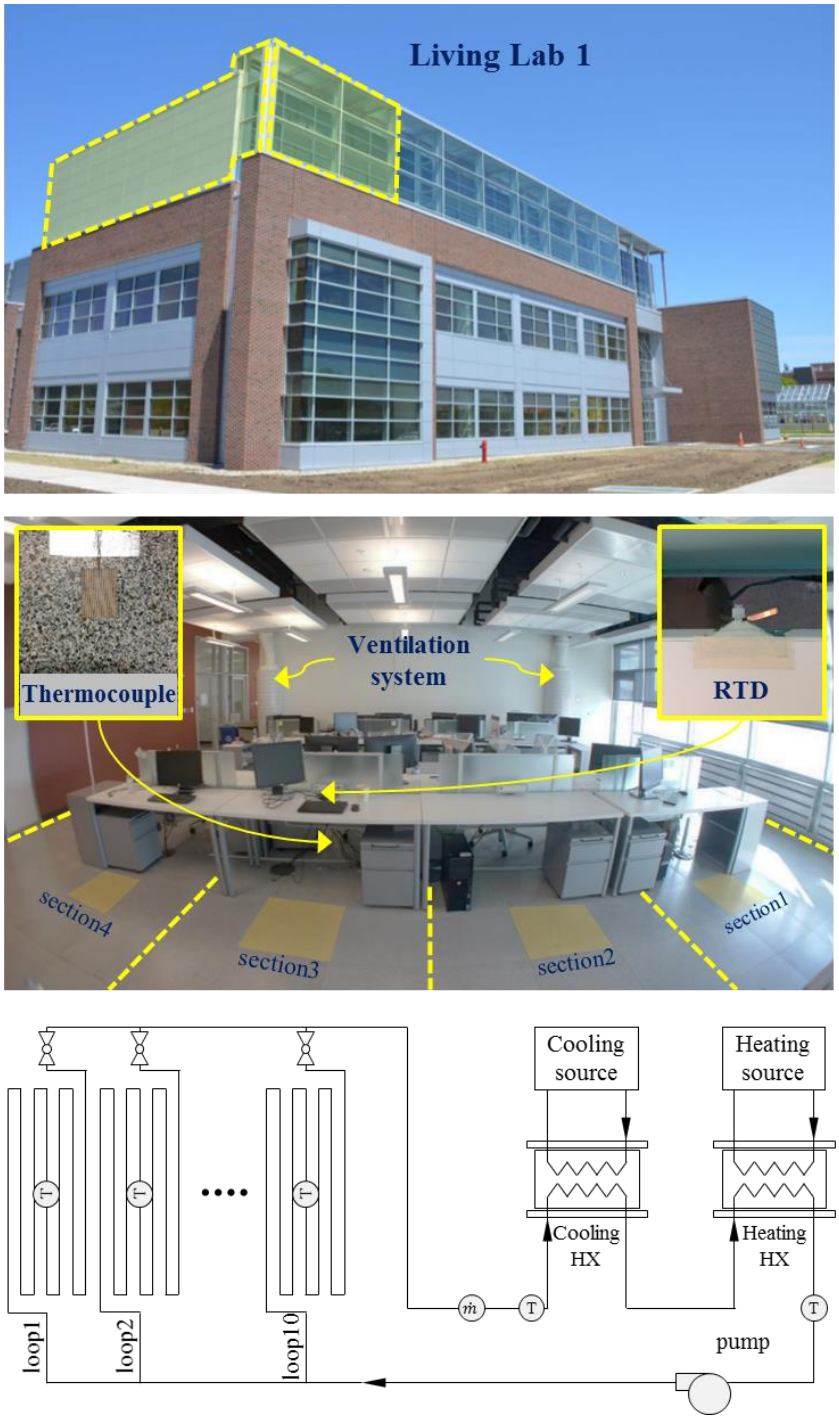

Figure 2 Exterior view of the test-building (top); interior fish eye view of living lab 1 (middle); pipe loops with heat exchanger (bottom).

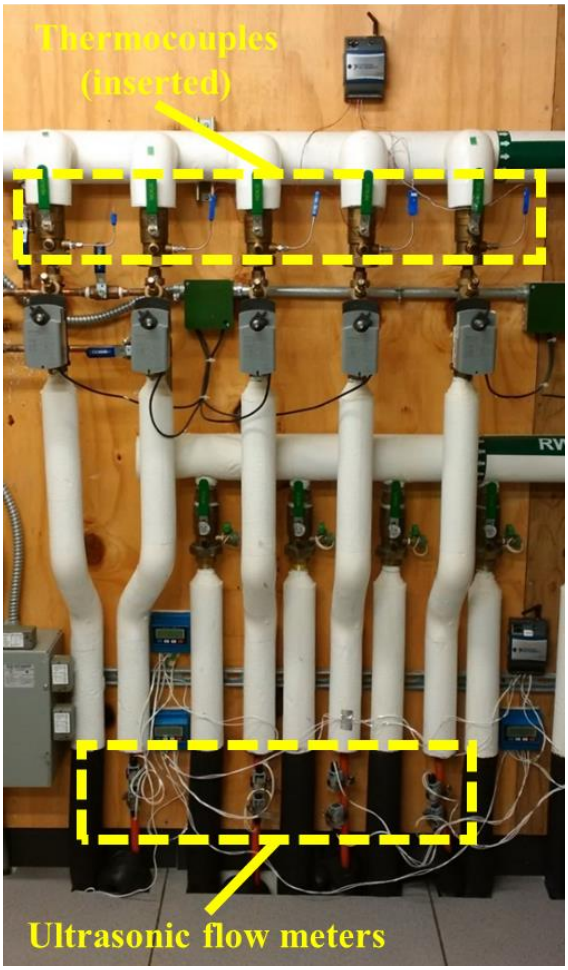

Figure 3 Pipe loops of the radiant floor system with temperature and flow meters installed.

according to the ventilation flow rate assuming the air is well-mixed since the wall-supply diffusers are distributed in four corners. The model structure of each thermal zone has one state and three or four resistances (1C3R or 1C4R). The radiant floor is treated as one agent. It consists of 12 states and 18 resistances (12C18R). The thermal capacity of each floor section is weighted with its area and the resistances between the four concrete sections ($R_{s,hor}$ and $R_{s,ver}$ in Figure 4(a)) are identical. Thus, the estimation is carried out with three states and three resistances to simplify the optimization problem. Internal heat gains from the equipment, occupants, and lighting are distributed to each section evenly. 90 % of equipment and occupant heat gain and 60% of lighting heat gain is an input the air node. The remaining portions (10 and 40% respectively) are inputs to the slab surface temperature node.

The initial unmeasured temperature state for the internal concrete nodes (T_{so} *and* T_{si}) is assumed to be the same with the slab surface temperature. Six optimizations run in parallel with six sub-system models (agents). This yields different values for the shared estimate parameters between sub-systems. The dual decomposition method (Algorithm 1) is used to iterate the solution of the optimization problem until the deviation of the shared parameters is less than 5% of their value, in which case, they are assumed to be

identical. Figure 5 shows the evolution of the shared parameters and reveals that 16 iterations are needed for the negotiation.

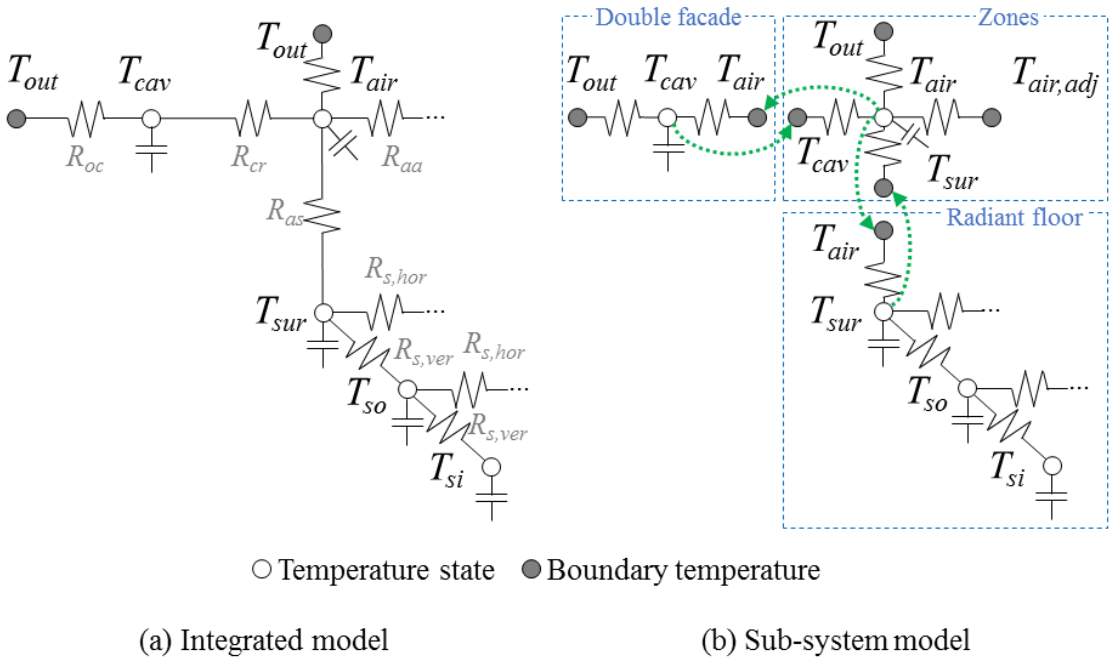

Figure 4. Integrated and sub-system model structure

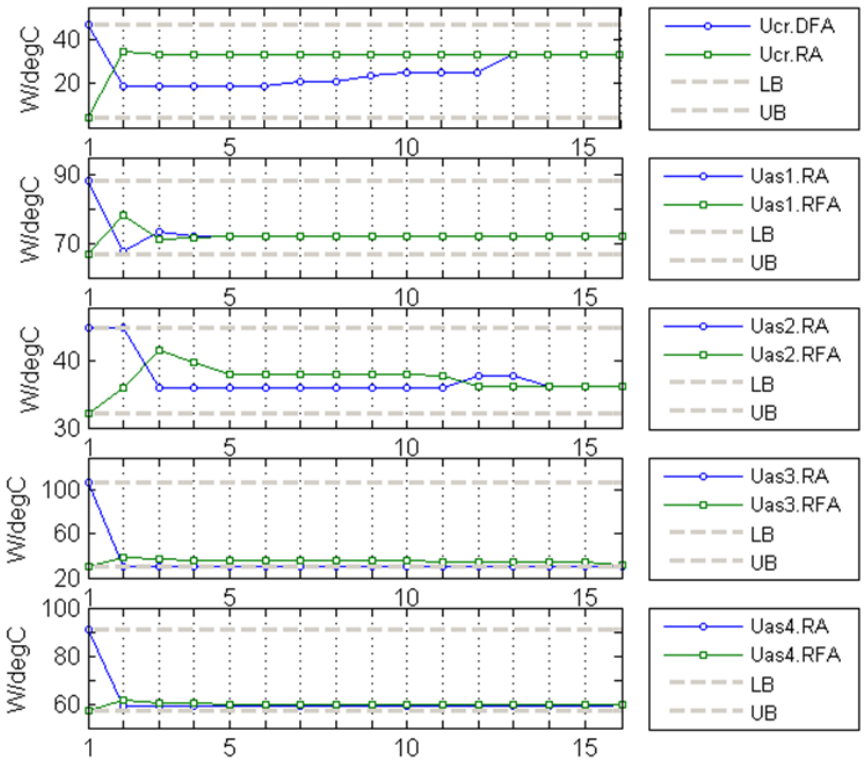

Figure 5. Evolution of shared parameters

Figure 6 shows results for one estimation set and two validation sets. Air and surface temperatures are shown on the left and right respectively along with the heat flux and temperature input at the bottom. The estimation period includes three days during which the radiant floor cooling system was ON and two days with free floating conditions. The Root Mean Square Error (RMSE) during the estimation period for the air and slab surface temperature in each section ranges from 0.43 to 0.58℃, and from 0.45 to 0.68℃, respectively. The model was validated with two different datasets as shown in Figures 6 (b) and (c). During this period, the radiant floor cooling system was ON in alternate sections for eight hours and free floating was used for four hours between turns. When this process was completed for all sections, another 12 hours of free floating was provided. Two cycles were used for the two different validation sets, respectively. For the first validation set, the RMSE of the air and slab surface temperature ranges from 0.55 to 0.82℃, and from 0.44 to 0.92℃, respectively (Figure 6 (b)). The corresponding ranges for the second validations set are 0.58 to 0.66℃, and 0.44 to 0.92℃ (Figure 6 (c)). This accuracy is considered to be reasonably good considering the complexity of the model.

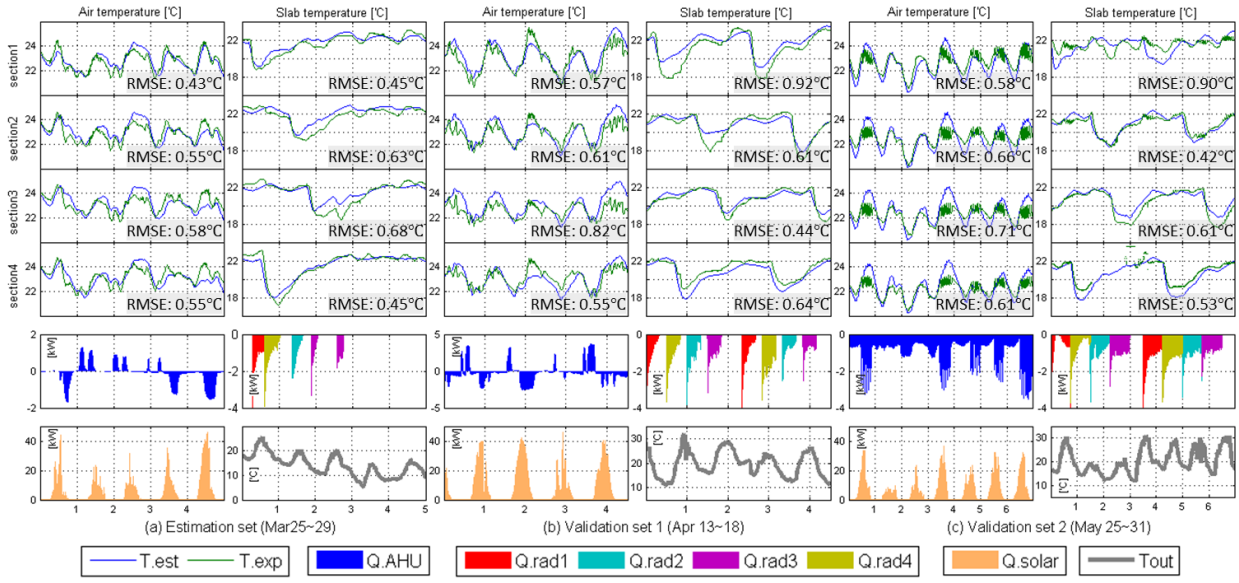

Figure 6. System identification results

3.3 DMPC implementation

3.3.1 HVAC system and objective function

An air-cooled chiller is considered as the HVAC source (Figure 7, left). The decision variable is the PLR of the chiller. The dimension of the controlled input vector is 48 for a 24hr prediction horizon with 30 min time-step. The electricity consumption of the chiller consists of the objective function with a regulation term as explained in Section 3.2 (Algorithm 2). The fan and pump electricity consumption is neglected, and the air system provides ventilation by regulating the supply air temperature to be equal to the average of the lower and upper temperature bounds. The initial control input trajectory $\mathbf{u}^0$ and multiplier

$\boldsymbol{\phi}^0$ are set to zero, and the step size and stop criteria (σ and ε_{stop} in Algorithm 2) are set to 50 and 0.0002. Performance data of the chiller are adopted from the EnergyPlus engineering reference [70] and the Energy Input Ratio (EIR) method is used based on the catalogue data of an actual product (Trane CGAM20). The nominal capacity ($Q_{ref,cap}$) and coefficient of performance ($C_{ref,COP}$) are 68.9 kW and 2.67, respectively [70]. For our case-study, the capacity is scaled down to 8 %. The electricity consumption of the chiller is a multiplication of three polynomials (f in Equation (5)) that represent the capacity, COP, and PLR. The capacity and COP curves are biquadratic and require two control inputs. The leaving water temperature ($T_{leaving}$) is fixed at 13 ℃ which yields a quadratic polynomial and the optimization problem has a convex form. The COP is plotted in Figure 7 (right) as a function of outdoor air temperature, leaving water temperature and PLR. Lower outdoor air temperature and higher leaving water temperature result in higher COP. As for the PLR, any ratio larger than 30% results in high COP.

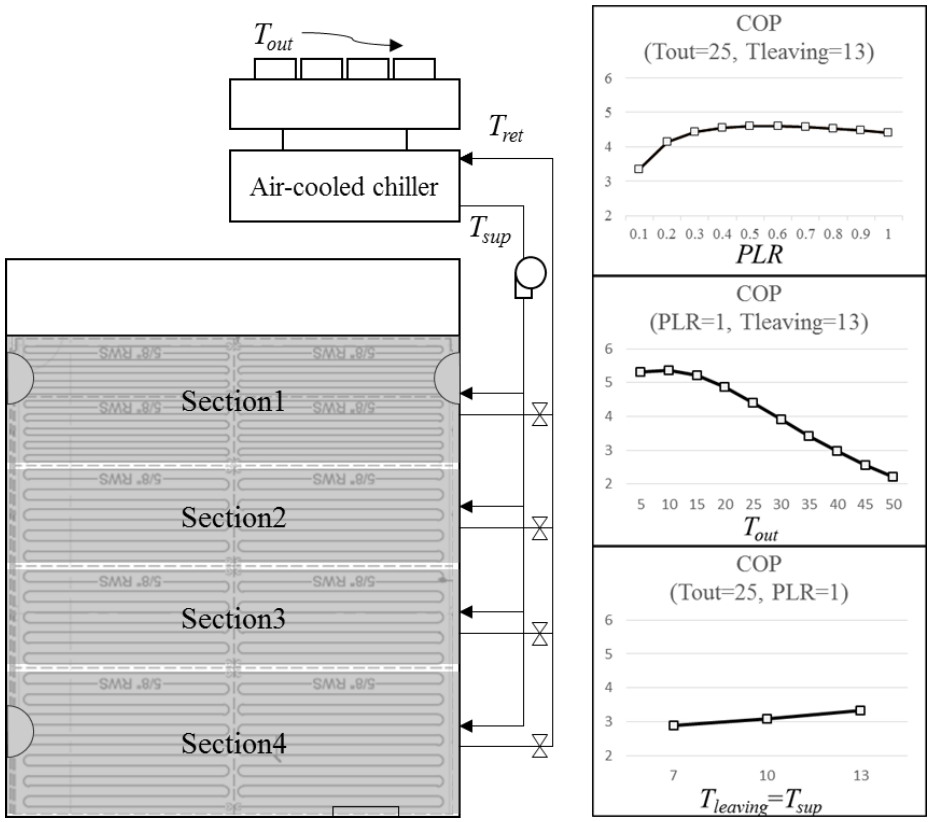

Figure 7. Test-bed with virtual air-cooled chiller (left) and Chiller performance curve (right)

$$
\begin{aligned}
& f_{chiller,n} = f_{Cap,n} \cdot f_{COP,n} \cdot f_{PLR,n} \\
& where: \begin{cases} f_{Cap,n} = Q_{ref,Cap} \cdot Curve_{biquad}\left(T_{leaving,n}, T_{outdoor,n}\right) \\ f_{COP,n} = \dfrac{1}{C_{ref,COP}} \cdot Curve_{biquad}\left(T_{leaving,n}, T_{outdoor,n}\right) \\ f_{PLR,n} = Curve_{quad}\left(\dfrac{Q_{load,n}}{f_{Cap,n}}\right) = Curve_{quad}\left(PLR_n\right) \end{cases}
\end{aligned} \tag{5}
$$

3.3.2 Optimization details: exogenous inputs and constraints

For the disturbance prediction, the occupant heat gain is set to 65 W for a sedentary working person based on ASHRAE Standard 55 [74]. The equipment heat gain for each occupant is calculated to be 50W based on measurements (historic data for weekends and weekdays) for the total power consumption and the actual number of occupants. The occupancy schedule is from 08 am to 10 pm considering the actual occupants of the test-bed. The operative temperature, which is a linear combination of the air and Mean Radiant Temperature, is used to control the space. It is calculated based on a weighted average of the air and slab temperature as the air flow rate in the zone is less than 0.2m/s [74]. For this purpose, a detailed experiment was conducted with an array of sensors including a globe meter and five thermocouples at various heights from the floor, to determine the two weighting coefficients. These are used in the actual MPC implementation for estimating the operative temperature (based on recommendations from ASHRAE 55 [74] using readings from the RTD sensor (at 0.6 m height from the ground) for the air temperature and from the thermocouple (TC) for the slab surface temperature (Figure 8). The weighting coefficients were estimated to be 0.77 for the air temperature and the 0.23 for the slab surface temperature. The RMSE between the experiment and estimation of the operative temperature is 0.12℃.

The vertical temperature difference between the head and ankle are used to quantify the thermal asymmetry [74]. This metric is used to define the limit of the maximum difference between the air and slab surface temperature which is set to be 7℃ based on recent studies with human test-subjects and a thermal manikin experiment [75, 76]. Also, the low bound of the slab surface temperature is set to 15℃ based on [77] to eliminate potential thermal discomfort of the occupants. This temperature bound for the floor affects the maximum cooling rate capacity of the radiant floor system as a large cooling rate is feasible when the concrete temperature is high and vice versa. Based on initial experiments, the maximum available cooling capacity for all floor slab sections was around 5kW when the slab surface temperature is 15℃ so this was set as an inequality constraint in the optimization problem. To eliminate violations of the operative temperature bounds, the valve is fully open to provide maximum cooling rate regardless of the cooling rate capacity limit when the actual operative temperature is higher than the upper temperature bound in each section.

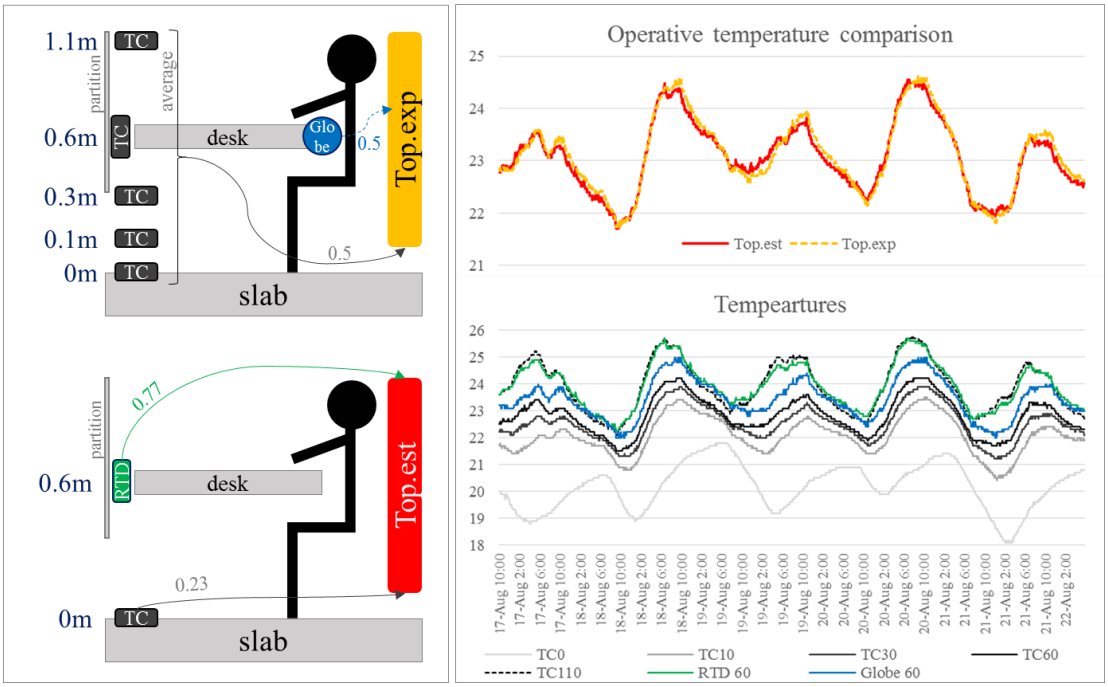

Figure 8. Experimental setting (left) and temperature profiles (right) for the operative temperature estimation

3.3.3 Data communication

A schematic for the DMPC implementation is shown in Figure 9. MPC calculations are performed in a server computer with Matlab that has access to weather forecast data for 24 hours prediction. The optimal cooling rate is calculated based on PLR and maximum chiller capacity ($f_{cap,n}$ in Eq (5)), and it is sent to Niagara server through Modbus communication. Then the valves for each section in the radiant floor cooling system are activated to satisfy the cooling rate signal in each loop for a given time-step, 30 min. After each time-step, sensor data for the zone and slab temperatures, the control and exogenous input are sent to the server computer, for the state estimation by the Kalman filter.

Weather forecast data including outdoor air temperature, relative humidity, and cloud cover are extracted from the National Oceanic and Atmospheric Administration (NOAA) web-site to a server computer. The following model was used for calculating the global horizontal irradiance (*GHI)* based on cloud cover forecast [78]:

$$GHI = I_0 \cdot \sin(h) \cdot \{C_0 + C_1(CC) + C_2(CC)^2 + C_3(T_{out(k)} - T_{out(k-3)}) + C_4(RH) + C_5 \cdot V_{wind}\} + d \quad (6).$$

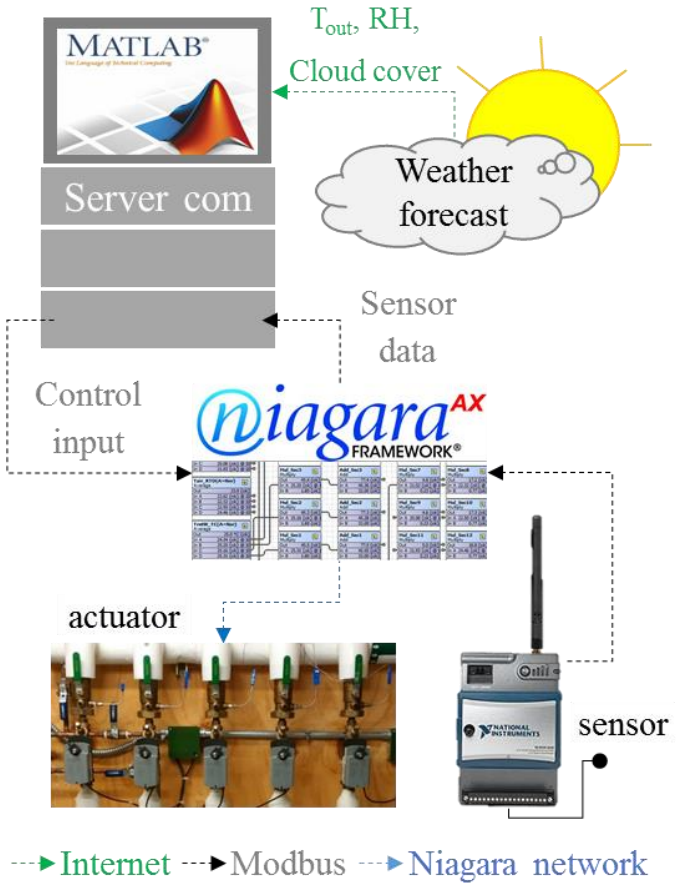

Figure 9. Data communication for MPC

GHI is calculated based on the solar constant (I_0, 1355 W/m^2), solar altitude angle (h), outdoor air temperature (T_{out}, k is time-step), cloud cover (CC), relative humidity (RH), wind speed (V_{wind}), and regression coefficients (C_0, C_1, C_2, C_3, C_4, C_5, and d) that are estimated for different climate zones in the literature [78]. Coefficients for zone Cfa (warm temperature, fully humid, and hot summer) were selected considering the location of the test-bed. Then the solar irradiance incident on the south façade is calculated from *GHI* using the *Solar Radiation Process* algorithm (Type 16 in TRNSYS) [71].

The initial states for the unmeasured temperatures are calculated with the Kalman filter [79]. The predicted error covariance (P in Eq 7) is updated from the previous time-step (P^-) with the state matrix (A_d) and the covariance matrix of process noise (Q) which is set based on the estimation results (averaged value of RMSE for the air and slab) in Section 4.2.The Kalman gain (K in Eq 8) is calculated with predicted error covariance and a covariance matrix of sensor noise (R in Eq 8) which is set based on temperature sensor accuracy. H is the matrix that extracts observed states from all states. Then the state (x) is updated based on the predicted state ($\hat{x}$) obtained from building dynamics (Eq 1) and the actual measurement (Y) along with the Kalman gain (Eq 9). Then the error covariance matrix (P^+) is updated to calculate the Kalman gain of the next iteration (Eq 10).

$$P = A_d P^- A_d^T + \mathrm{Q} \quad (7)$$

$$K = PH^T (HPH^T + \mathrm{R})^{-1} \quad (8)$$

$$x = \hat{x} + K(Y - H\hat{x}) \quad (9)$$

$$P^+ = (I - KH)P \quad (10)$$

In each time-step, multiple MPC calculations run sequentially until the convergence criteria is met. Although those computations run sequentially in a single server computer, parallel computing is realized as the information from other agents comes from the previous iterations. Therefore, the developed algorithm can be implemented in the future using new low-cost devices such as series of small single-board computers.

3.3.4 Implementation settings

Four phases were considered during the implementation with different settings for the operative temperature bounds as shown in Table 1. For the first two phases, relatively large temperature bounds were used to ensure proper operation of the system, while the bounds for phase 3 were significantly different among the different sections to evaluate the potential for localized thermal environment control. For phase 4, lower bounds were set to see if relatively low operative temperature preferences could be met.

Table 1. Lower and upper bounds of the operative temperature [℃]

	phase 1	phase 2	phase 3	phase 4
room section1	22.0~25.0	21.0~24.0	22.5~25.5	20.5~23.5
room section2	22.0~25.0	21.0~24.0	unoccupied	19.0~22.0
room section3	21.0~24.0	22.0~25.0	19.5~22.5	19.0~22.0
room section4	21.0~24.0	22.0~25.0	19.5~22.5	unoccupied

Figure 10 shows the implementation results for 11 consecutive days (September 16-26, 2017). The room air (Tar), slab surface (Tsl), and operative temperatures (Top) along with lower and upper bounds are shown for all sections along with the corresponding control and exogenous inputs. The gap on the graph for day 8 is due to data loss associated with a server communication failure. The operative temperature bounds for all sections are mostly satisfied for phase 1 and 2. Some exceedance hours due to upper bound violations are observed in phase 4. Although the operative temperature bounds are hard constraints in the optimization problem, the maximum cooling rate was provided occasionally when the temperature is violated.

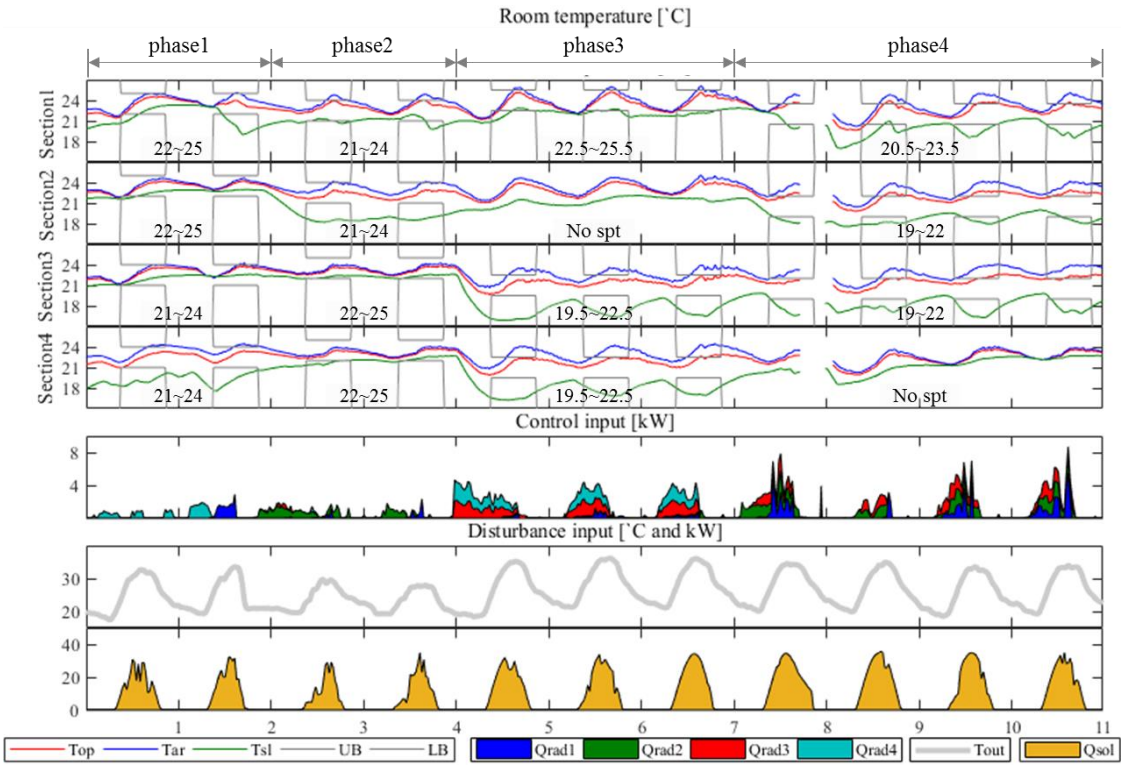

Figure 10. DMPC implementation results for four phases with different temperature bounds (September 16-26 2017)

3.4 Control performance analysis

In this section, results from the DMPC implementation in an actual test-bed are compared with simulations for two feedback and two MPC control strategies, introduced in Figure 11. The simulations are used for evaluating the performance of the DMPC algorithm and the DMPC controller. For feedback control, the room is considered to be represented by a single thermal zone and it is conditioned using a temperature bound that corresponds to the average of the values used in the four sections for the DMPC implementation (21.5~24.5, 20.5~23.5, and 19.5~22.5℃). For the first feedback controller (*Baseline-zone)*, all local sections are conditioned regardless of the occupancy unlike all the other cases in which localized conditioning is used for the occupied sections. The second feedback controller (*Baseline-local)* conditions only occupied sections. This comparison aims to investigate the energy saving potential of occupancy-based localized conditioning. To evaluate the DMPC algorithm, two simulation cases including CMPC and DMPC are used to investigate potential gaps between the theoretical and actual performance of the system. In simulation, MPC runs for each day and the last state is an input to the initial state for the next day so 11 consecutive MPCs run sequentially for 11days. The same disturbances for the weather and internal heat gain and algorithm settings, such as initial parameters ($\mathbf{u}^0$ and $\boldsymbol{\phi}^0$), step size (σ) and stop criteria (ε_{stop}), used in implementation were also used for the simulations.

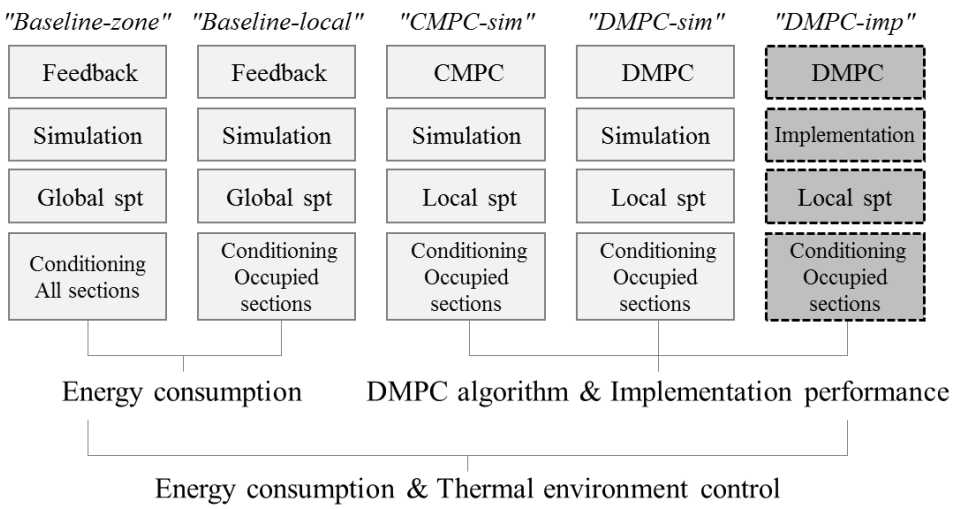

Figure 11. Different control scenarios used for the DMPC algorithm evaluation and the DMPC performance analysis

3.4.1 DMPC algorithm evaluation

Figure 12 shows the evolution of the objective function value and the residual for the regulation term of *DMPC sim*. Each line represents the optimization of one day. Residual represents the maximum value of the regulation term which is the deviation between the decision variables of the current and the previous iterations. Mostly, high fluctuations of the residual are seen for the initial iterations, and then they decrease. The algorithm requires13 to 157 iterations to converge which takes less than 5 min for each time-step which is sufficient for implementation in actual controllers, as the time-step for this study is 30 min.

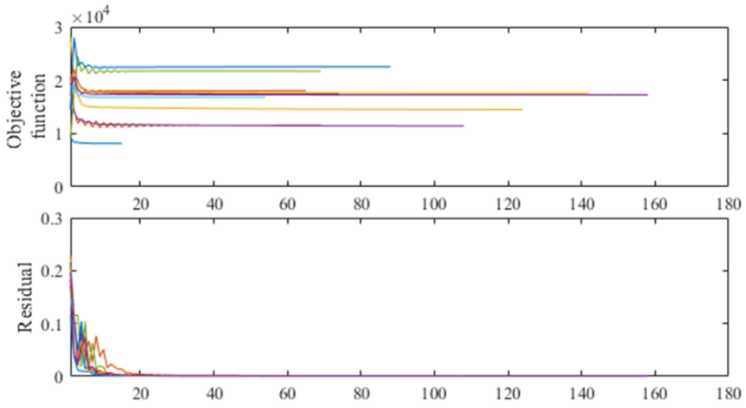

Figure 12. Evolution of objective function and residual in DMPC sim

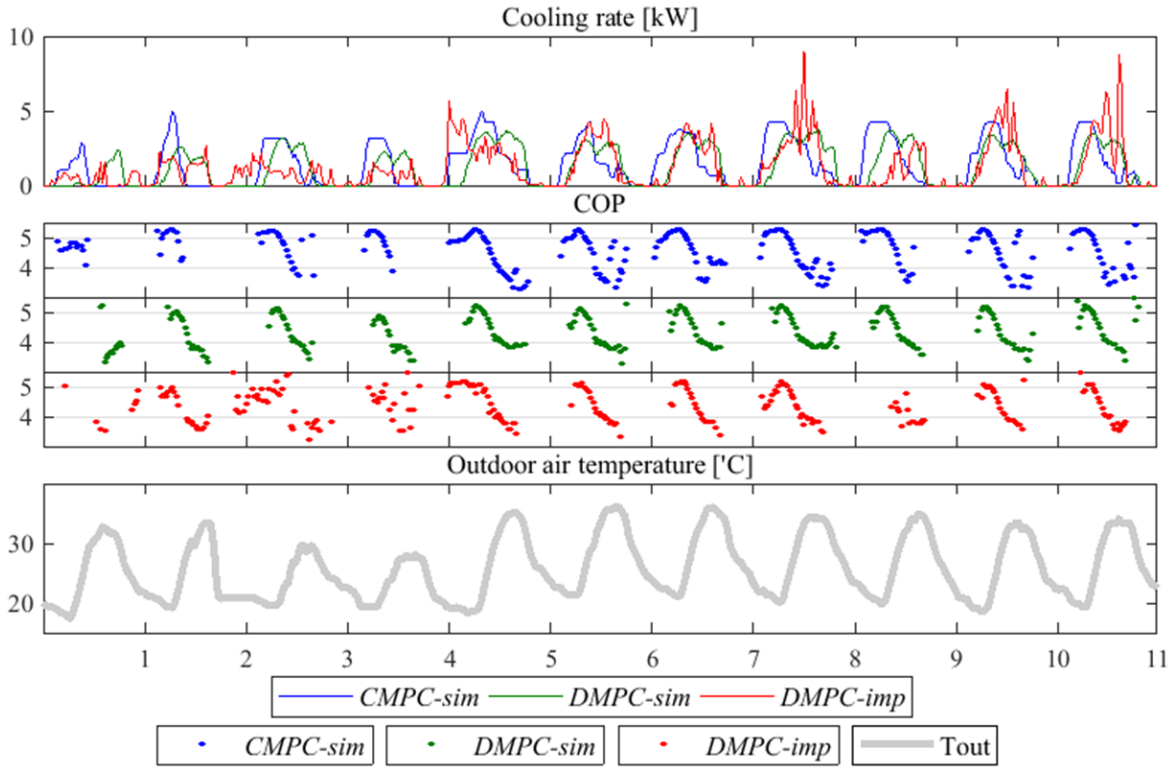

Figure 13. DMPC algorithm evaluation

Table 2. DMPC algorithm evaluation

Case	*CMPC-sim*	*DMPC-sim*	*DMPC-imp*
Cooling energy consumption[kWh]	350	327	314
Electricity consumption [kWh]	74	76	72

Figure 13 shows the cooling rate and COP variation during the test-period for the MPC simulations and DMPC implementation while Table 2 presents a summary of the results. Compared to CMPC, *DMPC-sim* results in lower cooling rate but higher electricity power consumption as the pre-cooling effect is less utilized. However, this compromise in DMPC controller performance is acceptable as the electricity consumption is increased by 2.8% only. As for the DMPC implementation, the cooling rate and electricity consumption is less compared to *DMPC-sim*; this is because the temperature bounds during implementation were not completely satisfied (see Section 4.3.4). Nevertheless, the pre-cooling effect is clearly seen with a higher COP and the total energy consumption is similar with the simulation; therefore, most of the potential benefits were captured in the implementation. If the room temperature would be perfectly regulated in implementation, the energy consumption would be the same with the simulation, which is a theoretical performance bound based on perfect disturbance prediction.

3.4.2 DMPC performance analysis

In this section, we investigate the energy saving potential of the occupancy-based control and DMPC by comparison with two feedback strategies. Table 3 shows the total cooling energy consumption

and electricity consumption. The occupancy-based localized feedback control (*baseline-local*) saves 4.8% compared to the *baseline-zone* for the specific occupant schedule presented in Table 1; the unoccupied period for the local sections is 84 hours, i.e.16% of the total. When the MPC is implemented using different set-points (temperature bound) and occupancy-based conditioning, which is *DMPC-imp*, around 27 % of electricity savings are possible compared to *Baseline-zone*. This is illustrated in Figure 14, which shows the operative temperature profiles with different bounds for all sections along with the cooling rate to the radiant floor and the COP variation. Compared to feedback control, DMPC utilizes pre-cooling so the chiller operates during the night or early in the morning to take advantage of the higher COP due to low outdoor air temperature. The variation of COP shows these distinct differences (Figure 14). Also, the MPC strategy itself saves 19 % of cooling energy (390 versus 314kWh) due to the large thermal capacity of the radiant floor system; as for the feedback control, cooling is provided from the slab to the room after the occupied hour.

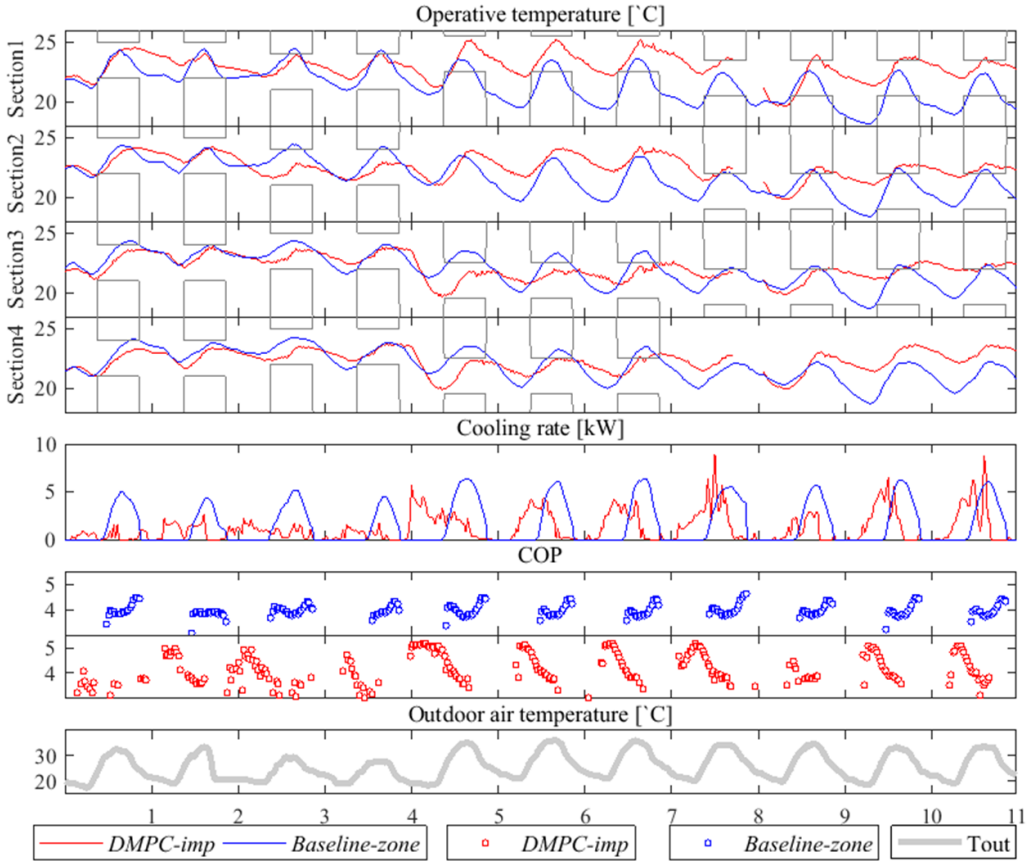

Figure 14. DMPC energy performance analysis

Table 3. DMPC energy performance analysis

Case	*Baseline-zone*	*Baseline-local*	*DMPC-imp*
Cooling energy consumption [kWh]	390	372	314
Electricity consumption [kWh]	99	94	72

The baseline feedback control *(Baseline-zone)* is compared with the *DMPC-sim* strategy that facilitates localized control based on different occupant preferences. The differences are quantified using the summation of operative temperature exceedance hours (℃·h) during occupancy and the results are presented in Table 4. For phase 1 and 2, the temperature exceedance with the *Baseline-zone* control is small because the temperature bounds of the different thermal zones are similar (21~24℃ and 22~25℃). However, when the bounds are significantly different (19.5~22.5 and 22.5~25.5℃ in phase 3; 19~22 and 20.5~23.5℃in phase 4), the temperature exceedance hours with the *Baseline-zone* control are increased. No temperature exceedance is observed in sections 2 and 4 for phase 3 and 4 as they were not occupied and thereby not conditioned. The total temperature exceedance hours for a period of 11 days are 75.3℃·h for the feedback control (*Baseline-zone*) and 22.2℃·h for *DMPC-imp*, i.e. 70.6% less. If different global temperature bounds such as the maximum or minimum value of the local bounds are implemented, the total exceedance hours of *Baseline-zone* are 191.3 or 45.6℃·h respectively which are still higher compared to *DMPC-imp*.

Table 4. Temperature exceedance comparison between Baseline-zone and DMPC-imp [℃·h]

	Baseline-zone				*DMPC-imp*			
	phase1	phase2	phase3	phase4	phase1	phase2	phase3	phase4
section1	0.4	1.2	10.1	1.6	0.2	0.0	1.1	2.5
section2	0.0	4.3	-	8.4	0.1	0.0	-	13.3
section3	2.2	0.0	20.9	7.0	0.0	0.0	0.0	3.8
section4	0.9	0.0	18.5	-	0.0	0.0	1.1	-

4 Discussion and conclusions

In this paper, we presented a multi-agent system approach for smart thermal environment control of office buildings. The developed algorithms were implemented in an actual test-bed with localized comfort delivery. The main findings and limitations are summarized as follows:

- The distributed system identification algorithm based on dual decomposition method yields building models with good prediction accuracy even for complex environments such as open-plan spaces with multiple individually controlled comfort delivery systems. The proposed method introduces building sub-system agents, which are optimized independently, by solving locally a nonlinear programming problem while the information is exchanged between the agents. Then, they are integrated into one model with further parallel optimizations by applying the dual decomposition method. This methodology can be extended to other building systems or different building scales, and could be packaged into a toolbox integrated in advanced open-source building control platforms (e.g., Voltron).

- The DMPC algorithm was implemented with the estimated building model and weather forecast. The control input for each radiant loop (agent) was calculated individually through the information exchange between agents and then provided to the actual BMS. The comparison with a centralized control approach shows that the DMPC algorithm captures most of the energy saving potential of the system. This approach is scalable so it can be generalized to larger scales of building systems such as multiple zones or building clusters. In this case, demand charge needs to be considered with electricity price information. Compared to feedback control, DMPC saves around 27% of the electricity consumption by utilizing the higher COP of the chiller through the pre-cooling period. At the same time, different thermal environments can be achieved by facilitating local conditioning in open-plan office spaces.

During the implementation, disturbance prediction such as occupant's schedule and internal heat gain profiles were estimated based on historical data. Also, the solar irradiance forecast is calculated with a deterministic model based on the climate zone of the actual test-bed. In future work, a more precise method for the solar irradiance forecast using site-specific data could be used (e.g. [80]), along with statistical methods for occupant's schedule [1, 2, 3, 4].

In this paper, we introduced scalable control functions and demonstrated localized thermal environment control in open-plan spaces using a radiant floor system with distributed sensing and data communication capabilities. Different comfort bounds are reported in the literature [75, 76, 81, 77] while recommendations for comfortable operative temperature ranges in ASHRAE 55 [74] might not be applicable for radiant floor systems. In the future, we will leverage on-going work on learning algorithms for occupants' thermal preferences [10, 16] and the research presented in this paper will be extended to integrate occupants' feedback in DMPC controllers.

In the case-study presented in this paper, a standard BMS system was used for the implementation of the DMPC algorithm. Although the MPC computations run sequentially in a single server computer, parallel computing is realized as the information from other agents comes from the previous iterations. In the future, the developed algorithm can be implemented using new low-cost devices such as series of small single-board computers. It is envisioned that smart building features with distributed sensing, occupant interaction, data communication and computing abilities could be widely adopted if intelligence is embedded into physical devices [67]. The research presented in this paper is the first step in this direction.

Acknowledgements

This work was funded by the National Science Foundation [grant number 1329875]. Any opinions, findings and conclusions or recommendations expressed in this material are those of the authors and do not necessarily reflect the views of the National Science Foundation. The authors would like to thank Prof. Jim

Braun (School of Mechanical Engineering, Purdue Univ.) and Prof. Jie Cai (Aerospace and mechanical engineering, Univ. of Oklahoma) for the fruitful discussions on this topic.

Nomenclature

A_d	state matrix in discretized state space formulation	–
B_d	input matrix in discretized state space formulation	–
C_d	output matrix in discretized state space formulation	–
C, d	constant for solar model	–
$\mathbf{C}$	matrix for mapping target state	–
f	polynomial equation for chiller performance	–
G	objective function in modelling	–
GHI	global horizontal solar irradiance	W/m^2
h	solar altitude angle	°
H	matrix for mapping observed states	–
K	Kalman gain	–
n	time-step	–
P	predicted error covariance	–
$\boldsymbol{q}$	control input vector in state space formulation	–
Q	covariance of process noise	–
Q	heat flux	W
R	covariance matrix of sensor noise	–
RH	relative humidity	%
T	temperature	℃
u	control input	–
$\mathbf{u}$	stacked control input matrix	–
V	wind speed	m/s
w	exogenous input	–
$\mathbf{w}$	stacked exogenous input matrix	–
$\boldsymbol{X}$	state vector in state space formulation	℃
y	temperature measurement	℃
$\hat{y}$	temperature prediction	℃
$\boldsymbol{\theta}$	estimate parameter	–
λ	Lagrangian multiplier for dual decompostion	–
μ	step-size for dual update	–
$\boldsymbol{\phi}$	convergence vector	–
$\boldsymbol{\sigma}$	time-step for convergence vector update	–
$\boldsymbol{\Omega}$	block matrix with state space formulation	–

References

01) Jia, Ruoxi, and Costas Spanos. 2016. “Occupancy Modelling in Shared Spaces of Buildings: A Queueing Approach.” *Journal of Building Performance Simulation* 0 (0). Taylor & Francis: 1–16. doi:10.1080/19401493.2016.1267802.

02) Liao, Chenda, and Prabir Barooah. 2010. “An Integrated Approach to Occupancy Modeling and Estimation in Commercial Buildings,” *Proceedings of the American Control Conference 2010*.

03) Yang, Zheng, Nan Li, Burcin Becerik-Gerber, and Michael Orosz. 2014. “A Systematic Approach to Occupancy Modeling in Ambient Sensor-Rich Buildings.” *Simulation 90 (8)*: 960–77. doi:10.1177/0037549713489918.

04) Zhang, Rui, Bing Dong, Burton Andrews, Khee Poh, Michael Ho, Yun-shang Chiou, and Diego Benitez. 2010. “An Information Technology Enabled Sustainability Test-Bed (ITEST) for Occupancy Detection through an Environmental Sensing Network.” *Energy & Buildings* 42 (7). Elsevier B.V.: 1038–46. doi:10.1016/j.enbuild.2010.01.016.

05) Zhao, Jie, Bertrand Lasternas, Khee Poh Lam, Ray Yun, and Vivian Loftness. 2014. “Occupant Behavior and Schedule Modeling for Building Energy Simulation through Office Appliance Power Consumption Data Mining.” *Energy & Buildings* 82. Elsevier B.V.: 341–55. doi:10.1016/j.enbuild.2014.07.033.

06) Bauman, F., H. Zhang, E. Arens, P. Raftery, C. Karmann, J. Feng, Y. Zhai, D. Dickerhoff, S. Schiavon, and X. Zhou. 2015. “Advanced Integrated Systems Technology Development: Personal Comfort Systems and Radiant Slab Systems.” Final report to CEC. June. www.escholarship.org/uc/item/88p8v7zb.

07) Pasut, Wilmer, Hui Zhang, Ed Arens, and Yongchao Zhai. 2015. “Energy-efficient Comfort with a Heated / Cooled Chair : Results from Human Subject Tests.” *Building and Environment 84*(2): 10–21. doi:10.1016/j.buildenv.2014.10.026.

08) Zhang, Hui, Edward Arens, and Yongchao Zhai. 2015. “A Review of the Corrective Power of Personal Comfort Systems in Non-Neutral Ambient Environments.” *Building and Environment* 91. Elsevier Ltd: 15–41. doi:10.1016/j.buildenv.2015.03.013.

09) Xu, Zhanbo, Shuo Liu, Guoqiang Hu, and Costas J. Spanos. 2017. “Optimal Coordination of Air Conditioning System and Personal Fans for Building Energy Efficiency Improvement.” *Energy and Buildings* 141. Elsevier B.V.: 308–20. doi:10.1016/j.enbuild.2017.02.051.

10) Lee, Seungjae, Panagiota Karava, Ilias Bilionis, and Athanasios Tzempelikos. 2018. “Inference of Thermal Preference Profiles for Personalized Thermal Environments.” ASHRAE winter conference.

11) Ryu, Minwoo, Jaeho Kim, and Jaeseok Yun. 2015. “Integrated Semantics Service Platform for the Internet of Things: A Case Study of a Smart Office.” Sensors (Switzerland) 15 (1): 2137–60. doi:10.3390/s150102137.

12) Weng, Thomas, and Yuvraj Agarwal. 2012. “From Buildings to Smart Buildings- Sensing and Actuation to Improve Energy Efficiency.” *IEEE Design & Test of Computers* 29 (4): 36–44. doi:10.1109/MDT.2012.2211855.

13) Jazizadeh, Farrokh, Ali Ghahramani, and Burcin Becerik-Gerber. 2013. “A Human-Building Interaction Framework for Personalized Thermal Comfort Driven Systems in Office Buildings.” *J. Comput. Civ. Eng.* 28 (1): 2–16. doi:10.1061/(ASCE)CP.1943-5487.0000300.

14) Jazizadeh, Farrokh, Ali Ghahramani, Burcin Becerik-gerber, Tatiana Kichkaylo, and Michael Orosz. 2014. “User-Led Decentralized Thermal Comfort Driven HVAC Operations for Improved Efficiency

in Office Buildings." *Energy & Buildings* 70. Elsevier B.V.: 398–410. doi:10.1016/j.enbuild.2013.11.066.

15) Konis, K., and M. Annavaram. 2017. "The Occupant Mobile Gateway: A Participatory Sensing and Machine-Learning Approach for Occupant-Aware Energy Management." *Building and Environment 118*. Elsevier Ltd: 1–13. doi:10.1016/j.buildenv.2017.03.025.

16) Lee, Seungjae, Ilias Bilionis, Panagiota Karava, and Athanasios Tzempelikos. 2017. "A Bayesian approach for probabilistic classification and inference of occupant thermal preferences in office buildings." *Building and Environment 118*. Elsevier Ltd: 323–343. doi:10.1016/j.buildenv.2017.03.009.

17) Stluka, Petr, Girija Parthasarathy, Steve Gabel and Tariq Samad, 2017. Chapter 2, Architectures and Algorithms for Building Automation—An Industry View.

18) Zhao, Peng, Therese Peffer, Ram Narayanamurthy, Gabe Fierro, Paul Raftery, Soazig Kaam, and Joyce Kim. 2016. "Getting into the Zone : How the Internet of Things Can Improve Energy Efficiency and Demand Response in a Commercial Building," *Proceeding of ACEEE Summer Study on Energy Efficiency in Buildings*. Pacific Grove, CA. August 21-26.

19) Hoyt, Tyler, Edward Arens, and Hui Zhang. 2014. "Extending Air Temperature Setpoints: Simulated Energy Savings and Design Considerations for New and Retrofit Buildings." *Building and Environment* 88. Elsevier Ltd: 89–96. doi:10.1016/j.buildenv.2014.09.010.

20) Baker, Lindsay, and Tyler Hoyt. 2016. "Control for the People : How Machine Learning Enables Efficient HVAC Use Across Diverse Thermal Preferences," *Proceedings of ACEEE Summer Study on Energy Efficiency in Buildings*. Pacific Grove, CA. August 21-26.1–8.

21) Erickson, Varick L, and Alberto E Cerpa. 2012. "Thermovote : Participatory Sensing for Efficient Building HVAC Conditioning." *Proceedings of the Fourth ACM Workshop on Embedded Sensing Systems for Energy-Efficiency in Buildings (BuildSys 12)*: 9–16.

22) Gao, Peter Xiang, and S Keshav. 2013. "Optimal Personal Comfort Management Using SPOT +." *Proceedings of the 5th ACM Workshop on Embedded Systems for Energy-Efficient Buildings (BuildSys 13)*: 1–8.

23) Gao, Peter Xiang, and S Keshav. 2013. "SPOT: a Smart Personalized Office Thermal Control System." *Proceedings of the fourth international conference on Future energy systems*: 237–246.

24) Heidarinejad, Mohammad, Daniel Alejandro Dalgo, Nicholas W Mattise, and Jelena Srebric. 2018. "Personalized Cooling as an Energy Efficiency Technology for City Energy Footprint Reduction." *Journal of Cleaner Production* 171. Elsevier Ltd: 491–505. doi:10.1016/j.jclepro.2017.10.008.

25) Vesely, Michal, and Wim Zeiler. 2014. "Personalized Conditioning and Its Impact on Thermal Comfort and Energy Performance - A Review." *Renewable and Sustainable Energy Reviews* 34. Elsevier: 401–8. doi:10.1016/j.rser.2014.03.024.

26) Zhang, Hui, Edward Arens, Dongeun Kim, Elena Buchberger, Fred Bauman, and Charlie Huizenga. 2010. "Comfort, Perceived Air Quality, and Work Performance in a Low-Power Task – Ambient Conditioning System." *Building and Environment* 45 (1). Elsevier Ltd: 29–39. doi:10.1016/j.buildenv.2009.02.016.

27) Amai, Hideyuki, Shin-ichi Tanabe, Takashi Akimoto, and Takeshi Genma. 2007. "Thermal Sensation and Comfort with Different Task Conditioning Systems" 42: 3955–64. doi:10.1016/j.buildenv.2006.07.043.

28) Kong, Meng, Thong Q. Dang, Jianshun Zhang, and H. Ezzat Khalifa. 2017. "Micro-Environmental Control for Efficient Local Cooling." *Building and Environment* 118. Elsevier Ltd: 300–312. doi:10.1016/j.buildenv.2017.03.040.

29) Vissers, Derek. 2012. "The Human Body as Sensor for Thermal Comfort Control," Master thesis. Eindhoven University of Technology.

30) Andersen, M., G. Fierro, S. Kumar, J. Kim, E. Arens, H. Zhang, P. Raftery, and D. Culler. 2016. "Well-connected microzones for increased building efficiency and occupant comfort." *Proceedings of ACEEE Summer Study on Energy Efficiency in Buildings*. Pacific Grove, CA. August 21-26.

31) Schiavon, Stefano, Kwang Ho Lee, Fred Bauman, and Tom Webster. 2011. "Simplified Calculation Method for Design Cooling Loads in Underfloor Air Distribution (UFAD) Systems." *Energy and Buildings* 43(2-3): 517-528. doi:10.1016/j.enbuild.2010.10.017.

32) Foda, Ehab, and Kai Sirén. 2012. "A Thermal Manikin with Human Thermoregulatory Control: Implementation and Validation." *International Journal of Biometeorology* 56 (5). Elsevier B.V.: 959–71. doi:10.1007/s00484-011-0506-6.

33) Fabrizio, Enrico, Stefano P. Corgnati, Francesco Causone, Marco Filippi. 2012. "Numerical comparison between energy and comfort performance of radiant heating and cooling systems versus air systems." *HVAC&R Research* 18(4).

34) Nall, D. H. 2013. "Thermally active floors: Part1." ASHRAE Journal, 55(1).

35) Nall, D. H. 2013. "Thermally active floors: Part2." ASHRAE Journal, 55(2).

36) Nall, D. H. 2013. "Thermally active floors: Part3." ASHRAE Journal, 55(3).

37) Rhee, Kyu-Nam. and Kwang Woo. Kim. 2015. "A 50 year review of basic and applied research in radiant heating and cooling systems for the built environment." *Building and Environment* 91: 640–650.

38) Rhee, Kyu-nam, Bjarne W Olesen, and Kwang Woo Kim. 2017. "Ten Questions about Radiant Heating and Cooling Systems." *Building and Environment* 112. Elsevier Ltd: 367–81. doi:10.1016/j.buildenv.2016.11.030.

39) Bengea, Sorin C., Anthony D. Kelman, Francesco Borrelli, Russell Taylor, and Satish Narayanan. 2014. "Implementation of Model Predictive Control for an HVAC System in a Mid-Size Commercial Building." *HVAC&R Research* 20 (February 2014): 121–35. doi:10.1080/10789669.2013.834781.

40) Sourbron, Maarten, Clara Verhelst and Lieve Helsen. 2013. "Building models for model predictive control of office buildings with concrete core activation." *Journal of Building Performance Simulation* 6(3): 175–198.

41) Váňa, Zdeněk, Jiří Cigler, Jan Široký, Eva Žáčeková, and Lukáš Ferkl. 2014. "Model-Based Energy Efficient Control Applied to an Office Building." *Journal of Process Control* 24 (6): 790–97. doi:10.1016/j.jprocont.2014.01.016.

42) Feng, Jingjuan (Dove), Frank Chuang, Francesco Borrelli, and Fred Bauman. 2015. "Model Predictive Control of Radiant Slab Systems with Evaporative Cooling Sources." *Energy and Buildings* 87 (January): 199–210. doi:10.1016/j.enbuild.2014.11.037.

43) Braun, J. E., 1990. "Reducing energy costs and peak electrical demand through optimal control of building thermal storage." *ASHRAE transactions* 96(2), 876–888.

44) Oldewurtel, Frauke, Alessandra Parisio, Colin N. Jones, Dimitrios Gyalistras, Markus Gwerder, Vanessa Stauch, Beat Lehmann, and Manfred Morari. 2012. "Use of Model Predictive Control and

Weather Forecasts for Energy Efficient Building Climate Control." *Energy and Buildings* 45 (2): 15–27. doi:10.1016/j.enbuild.2011.09.022.

45) Joe, Jaewan, and Panagiota Karava. 2016. "Agent-Based System Identification for Control-Oriented Building Models." *Journal of Building Performance Simulation*. Taylor & Francis: 1–22. doi:10.1080/19401493.2016.1212272.

46) Cai, Jie, James E Braun, Donghun Kim, Rita Jaramillo, and Jianghai Hu. 2016. "A Multi-Agent Control Based Demand Response Strategy for multi-zone buildings." *Proceedings of the American Control Conference 2016*-July. doi:10.1109/ACC.2016.7525271.

47) Ma, Yudong, Anthony Kelman, Allan Daly, and Francesco Borelli. 2012. "Predictive Control for Energy Efficient Buildings with Thermal Storage." *IEEE Control Systems*, no. February: 44–64. doi:10.1109/MCS.2011.2172532.

48) Jennings, N.R., and S. Bussmann. 2003. "Agent-Based Control Systems: Why Are They Suited to Engineering Complex Systems?" *IEEE Control Systems* 23 (3): 61–73. doi:10.1109/MCS.2003.1200249.

49) Necoara, Ion, Valentin Nedelcu, and Ioan Dumitrache. 2011. "Parallel and Distributed Optimization Methods for Estimation and Control in Networks." *Journal of Process Control* 21 (5): 756–66. doi:10.1016/j.jprocont.2010.12.010.

50) Negenborn, R.R., and J.M. Maestre. 2014. "Distributed Model Predictive Control: An Overview and Roadmap of Future Research Opportunities." *IEEE Control Systems* 34 (August): 87–97. doi:10.1109/MCS.2014.2320397.

51) Samar, S, Stephen Boyd, and Dimitry Gorinevsky. 2007. "Distributed Estimation via Dual Decomposition." *Proc. European Control Conference*, 1511–16. https://www.stanford.edu/~boyd/papers/pdf/distr_estim_ecc.pdf.

52) Zhao, Peng, Siddharth Suryanarayanan, and Marcelo Godoy Simões. 2013. "An Energy Management System for Building Structures Using a Multi-Agent Decision-Making Control Methodology." *IEEE Transactions on Industry Applications* 49 (1): 1–9. doi: 10.1109/IAS.2010.5615412.

53) Simoes, M Godoy, and Saurav Bhattarai. 2011. "Multi Agent-based Energy Management Control for Commercial Buildings." *2011 IEEE Industry Applications Society Annual Meeting*, 1–6. doi:10.1109/IAS.2011.6074360.

54) Wang, Zhu, Rui Yang, and Lingfeng Wang. 2010. "Multi-Agent Control System with Intelligent Optimization for Smart and Energy-Efficient Buildings." *IECON Proceedings (Industrial Electronics Conference)*, 1144–49. doi:10.1109/IECON.2010.5675530.

55) Lacroix, Benoit, Liten Ines, and David Mercier. 2012. "Multi-Agent Control of Thermal Systems in Buildings." *Agent Technology for Energy Systems Workshop (ATES 2012)*.

56) Davidsson, Paul, and Magnus Boman. 2005. "Distributed Monitoring and Control of Office Buildings by Embedded Agents." *Information Sciences* 171 (4): 293–307. doi:10.1016/j.ins.2004.09.007.

57) Duan, Jianmin, and Fan Lin. 2008. "Research of Intelligent Building Control Using an Agent-Based Approach." *2008 6th IEEE International Conference on Industrial Informatics*, 991–94. doi:10.1109/INDIN.2008.4618246.

58) Mo, ZhengChun and Ardeshir Mahdavi. 2003. "An agent-based simulation-assisted approach to bi-lateral building systems control." *Proceedings of the International IBPSA conference*. Eindhoven, Netherlands, 887–894.

59) Camponogara, Eduardo, Dong Jia, Bruce H Krogh, and Sarosh Talukdar. 2002. "Distributed Model Predictive Control" *IEEE Control Systems* 22 (1): 44–52. doi: 10.1109/37.980246.

60) Christofides, Panagiotis D., Riccardo Scattolini, David Munoz de la Pena, and Jinfeng Liu. 2013. "Distributed Model Predictive Control: A Tutorial Review and Future Research Directions." *Computers and Chemical Engineering* 51: 21–41. doi:10.1016/j.compchemeng.2012.05.011.

61) Moroşan, Petru-Daniel, Romain Bourdais, Didier Dumur, and Jean Buisson. 2010. "Building Temperature Regulation Using a Distributed Model Predictive Control." *Energy and Buildings* 42 (9): 1445–52. doi:10.1016/j.enbuild.2010.03.014.

62) Lamoudi, Mohamed Yacine, Mazen Alamir & Patrick Béguery. 2011. "Distributed constrained Model Predictive Control based on bundle method for building energy management." *Proceedings of 50th IEEE Conference on Decision and Control and European Control Conference (CDC-ECC)*: 8118–8124.

63) Pflaum, Peter, Mazen Alamir, & Mohamed Yacine Lamoudi. 2014. "Comparison of a primal and a dual decomposition for distributed MPC in smart districts," *Proceedings of IEEE International Conference on Smart Grid Communications*: 55–60.

64) Koehler, Sarah, and Francesco Borrelli. 2013. "Building Temperature Distributed Control via Explicit MPC and 'Trim and Respond' Methods." *Control Conference (ECC)*: 4334–39. http://ieeexplore.ieee.org/xpls/abs_all.jsp?arnumber=6669781.

65) Ma, Yudong, Garrett Anderson, and Francesco Borrelli. 2011. "A Distributed Predictive Control Approach to Building Temperature Regulation." American Control Conference, 2089–94. doi:10.1109/ACC.2011.5991549.

66) Ma, Yudong, Stefan Richer, and Francesco Borrelli. 2012. *Control and Optimization with Differential-Algebraic Constraints: DMPC for Building Temperature Regulation*. SIAM. doi:10.1137/9781611972252.ch14.

67) Cai, Jie, Donghun Kim, Rita Jaramillo, James E Braun, and Jianghai Hu. 2016. "A General Multi-Agent Control Approach for Building Energy System Optimization." *Energy & Buildings* 127. Elsevier B.V.: 337–51. doi:10.1016/j.enbuild.2016.05.040.

68) Cai, Jie, James E Braun, Donghun Kim, and Jianghai Hu. 2016. "General Approaches for Determining the Savings Potential of Optimal Control for Cooling in Commercial Buildings Having Both Energy and Demand Charges." *Science and Technology for the Built Environment* 22(6): 733–750, DOI: 10.1080/23744731.2016.1197716.

69) Hou, Xiaodong, Yingying Xiao, Jie Cai, Jianghai Hu, and James E Braun. 2016. "A Distributed Model Predictive Control Approach for Optimal Coordination of Multiple Thermal Zones in a Large Open Space." *International high performance buildings conference*, Purdue University, West Lafayette, July 11–14.

70) EnergyPlus. 2015. EnergyPlus engineering reference: the reference to EnergyPlus calculations. Lawrence Berkel0)ey National Laboratory.

71) TRNSYS 18. 2017. http://sel.me.wisc.edu/trnsys/.

72) MathWorks. 2014. Optimization Toolbox™ User's Guide.

73) Tridium Inc. Niagara AX Software. http://www.tridium.com/.

74) ASHRAE, ANSI/ASHRAE Standard 55-2013, Thermal comfort Conditions for Human Occupancy, ASHRAE, Atlanta, 2013.

75) Krajčík, Michal, Roberta Tomasi, Angela Simone, and Bjarne W. Olesen. 2013. "Experimental Study Including Subjective Evaluations of Mixing and Displacement Ventilation Combined with Radiant Floor Heating/cooling System." *HVAC and R Research* 19 (8): 1063–72. doi:10.1080/10789669.2013.806173.

76) Krajčík, Michal, Roberta Tomasi, Angela Simone, and Bjarne W. Olesen. 2016. "Thermal Comfort and Ventilation Effectiveness in an Office Room with Radiant Floor Cooling and Displacement Ventilation." *Science and Technology for the Built Environment* 22 (3): 317–27. doi:10.1080/23744731.2016.1131568.

77) Wang, R. Z., Zhang H, Arens E, D Lehrer, C Huizenga, S Hoffman, and Yu.T. 2009. "Modeling the Thermal Comfort with Radiant Floors and Ceilings." *4th International Building Physics Conference 2009*. June 15–18.

78) Seo, Donghyun. 2010. "Development of a universal model for predicting hourly solar radiation—Application: Evaluation of an optimal daylighting controller." PhD thesis. University of Colorado.

79) Robert F. Stengel. Optimal control and estimation. 1994.

80) Liu, Xiaoqi, Parth Paritosh, Nimish Awalgaonkar, Ilias Bilionis, and Panagiota Karava. 2018. "Model predictive control under forecast uncertainty for optimal operation of buildings with integrated solar systems." submitted to *Solar Energy*.

81) Nevins, Ralph G., and A. M. Feyerherm. 1967. "Effect of Floor Surface Temperature on Comfort Part - Part IV: Cold Floors." *ASHRAE Transactions*.